

# Organic Nanowire Single-Mode Laser from a Hybrid Bound State in the Continuum

Yuan Li,<sup>||</sup> Jiajun Wang,<sup>||</sup> Kai Wang, Chunling Gu,<sup>\*</sup> Hongbing Fu,<sup>\*</sup> Lei Shi,<sup>\*</sup> and Qing Liao<sup>\*</sup>Cite This: <https://doi.org/10.1021/acsphotonics.5c02055>

Read Online

ACCESS |



Metrics &amp; More

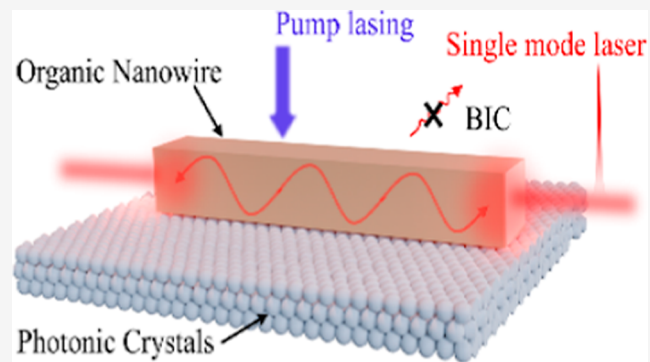


Article Recommendations



Supporting Information

**ABSTRACT:** Nanoscale single-mode lasers are a class of excellent coherent light sources for future on-chip integrated photonic circuits due to their high monochromaticity and beam quality. However, the lasing of the desired mode cannot completely prevent neighboring resonances because of the competition between the broad gain bandwidth of materials and the free spectral range. In this study, we have employed the high-quality characteristics of the bound state in the continuum (BIC) to successfully realize the desired single-mode lasing emission from a large-sized organic nanowire on the three-dimensional photonic crystal (PhC) substrate. Benefited from the tunability of PhCs, the wavelength of single-mode laser can be effectively regulated due to the pronounced periodicity-dependent characteristics of BICs. Importantly, this device exhibits a robust single-mode laser due to the immunity of the defects of PhCs. Our experimental finding offers significant insights for developing synthetic lasing devices toward



next-generation optoelectronic integrated devices.

**KEYWORDS:** single-mode laser, organic nanowire, photonic crystal, bound state in the continuum

## 1. INTRODUCTION

Nanoscale chip-integrable coherent light sources are fundamental optical components for future integrated photonic circuits.<sup>1</sup> Compared to the mature and commercially available inorganic lasers based on III–V compounds and similar materials,<sup>2</sup> organic lasers (including ONWLs) offer a new research platform for constructing nanoscale coherent light sources. This is enabled by their distinct advantages: a broad material library, strong waveguiding effects, high optical gain, and subwavelength diameters.<sup>3–7</sup> Notably, their excellent solution processability provides distinct advantages for flexible and large-area fabrication, demonstrating long-term potential to address specific application challenges such as flexible integration and customized wavelength requirements.<sup>8,9</sup> One of the primary goals of designing ONWLs is to operate in a single mode and high brightness due to the advantages of their high monochromaticity and beam quality. However, there is a natural challenge between high-brightness and single-mode laser because high brightness lasers require large optical dimensions while single-mode operation needs small dimensions for offering large free spectral range (FSR). Thus, achieving single-mode operation in large-size organic nanowires is very difficult because the broad gain bandwidth and small FSR stem from large dimensions. Several approaches have been developed to pursue single-mode operation, such as parity-time symmetry breaking,<sup>10–12</sup> additional coupled cavity for the Vernier effect,<sup>13,14</sup> enlarged FSR through mode size

reduction,<sup>15,16</sup> distributed feedback gratings or distributed Bragg reflector,<sup>17,18</sup> and topological laser device.<sup>19,20</sup> However, not all of these approaches are practically compatible with the manufacturing processes, and each of them introduces extra demands in terms of specific configurations and fabrication complexity. Therefore, identifying an alternative strategy for achieving single-mode operating lasers is extremely desired.

Bound states in the continuum (BICs),<sup>21–24</sup> benefited from their infinite quality ( $Q$ ) factor and strict confinement of light,<sup>25–27</sup> are emerging as a powerful tool for achieving high-stability, low-threshold, and high-output-power lasers. Some successful efforts for BIC lasers have been demonstrated in surface-emitting inorganic lasers by means of suppressing out-of-plane radiations and boosting the  $Q$  factors of planar optical resonators.<sup>28–33</sup> However, most reports on BIC lasers have focused on 2D optical gain materials, which are not compatible with nanowire geometries. Integrating robust BICs into a nanowire laser to achieve single-mode lasers remains a critical challenge.

**Received:** August 28, 2025

**Revised:** November 26, 2025

**Accepted:** November 26, 2025

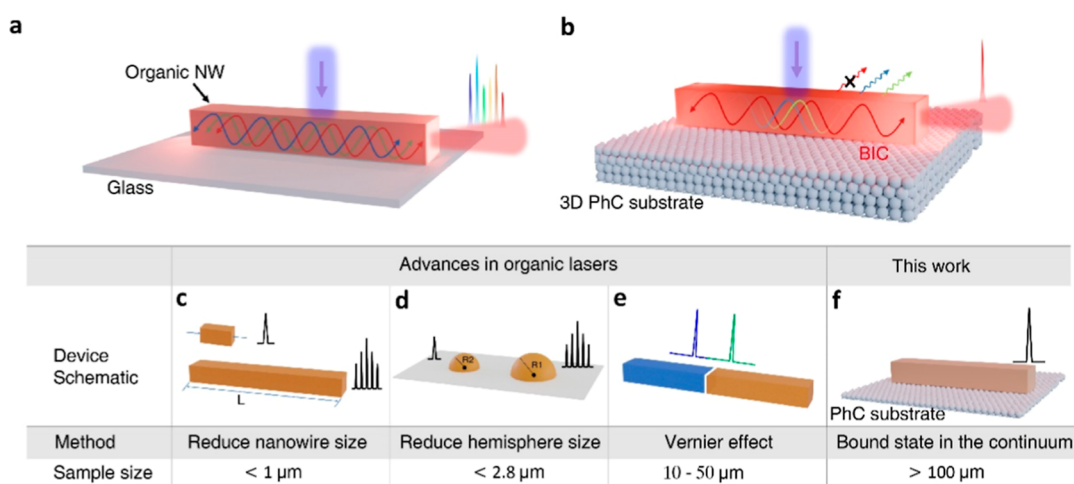


**Figure 1.** Schematic diagram of organic nanowire lasers operating in the multimode (a) and single-mode regime (b), respectively. Advances in organic lasers (c–e) and this work (f).

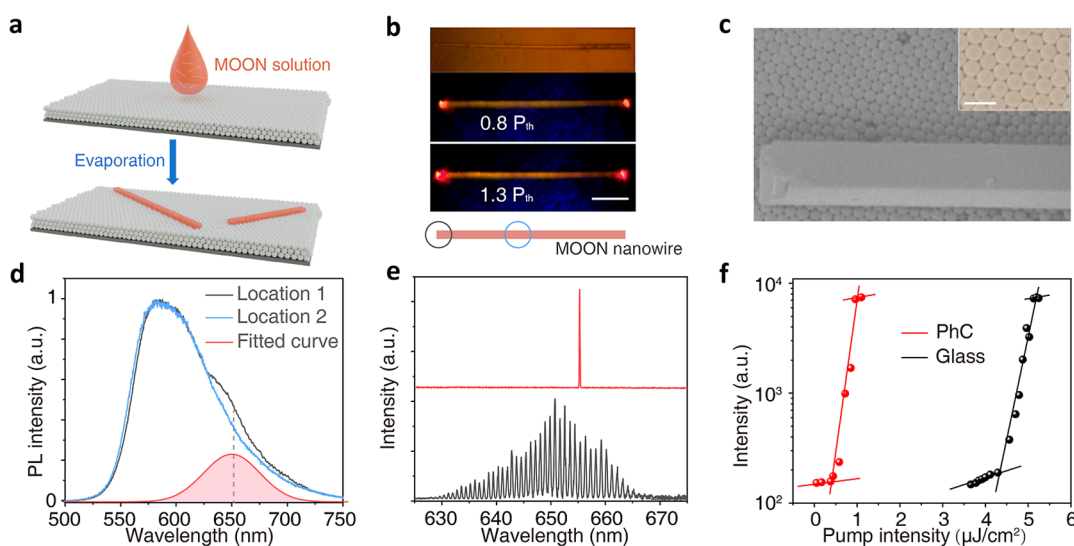


**Figure 2.** (a) The schematic of the preparation process of the composite system. The MOON nanowires formed after the solvent was evaporated on the PhC. (b) The images of the composite system below and above the threshold. Scale bars: 20  $\mu\text{m}$ . Black and blue circle represent the test location at the edge and middle of the nanowires, respectively. (c) SEM image of a MOON nanowire on the PhC. The inset shows the amplified image with the scale bar of 600 nm. (d) The PL spectra measured at the edge and the middle of the nanowire, respectively. (e) The lasing spectra of the MOON nanowire on the glass substrate (black line) and PhC substrate (red line). (f) The threshold curves of the MOON nanowire on the glass substrate (black line) and PhC substrate (red line).

In this study, we realize a low-threshold and robust single-mode organic nanowire laser by means of a hybrid BIC mechanism regardless of the large dimensions of the organic nanowires, where the proposed “hybrid BIC” emerges from the coupling between the organic nanowire’s waveguide mode and the photonic crystal (PhC) substrate. This synergistic interaction creates a high- $Q$  bound state that preserves traditional BIC radiation suppression while inheriting organic nanowires’ excellent gain and low-threshold properties. For the construction of our laser devices, the obtained organic nanowires are simply placed onto a three-dimensional (3D) PhC substrate. BICs of the composite structures are crucial in the selective enhancement of the specific laser modes. The single-mode lasing from the composite device structure has been achieved. Besides the mode selection, the threshold of the single-mode laser has been reduced by 10 times compared to that of the individual nanowire laser. Benefited from the tunability of PhCs, the wavelength of single-mode laser can be

effectively regulated due to the pronounced periodicity-dependent characteristics of BICs. Importantly, this device exhibits a robust single-mode laser due to the immunity of the defects of 3D PhCs. Our results not only shed light on the underlying physics of BICs but also offer significant insights for developing synthetic lasing device toward next-generation optoelectronic integrated devices.

## 2. RESULTS AND DISCUSSION

Organic microcrystals with regular morphologies can support lasing emission due to their excellent resonant cavity and optical gain.<sup>3–5</sup> For the common organic microcrystals, lasing emission usually operates in the multimode regime due to the FSR being much smaller than the gain bandwidth of the gain medium. Typically, the nanowire employs Fabry-Pérot cavity to generate multimode laser due to the large longitudinal dimension (Figure 1a). Reducing the dimensions of the

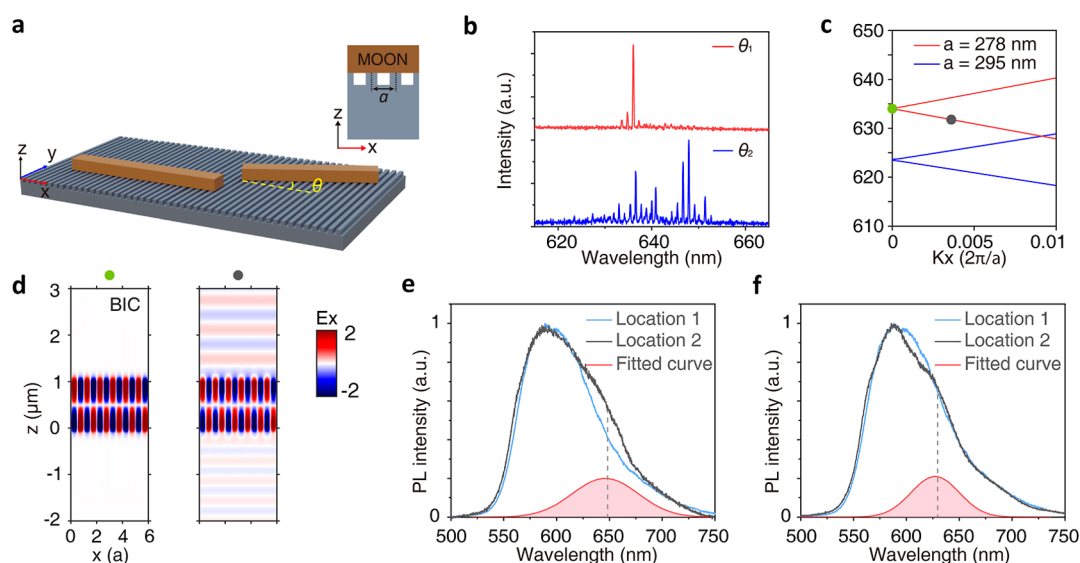


**Figure 3.** (a) Schematic of the nanowire on the 1D PhC grating.  $a$  is the period. (b) Laser spectra of the acquired nanowire at periods of 278 and 295 nm. (c) Photonic bands of the grating-organic crystal composite structure at periods of 278 nm (red line) and 295 nm (blue line). (d) Distributions of  $x$ -component electric field ( $E_x$ ) for the optical modes in (c). (e, f) Spectral changes measured at the edge and in the middle of the nanowire with a period of 278 and 295 nm.

crystals is a general solution, but it leads to an increase in the laser threshold and the decrease in the laser intensity (Figure 1c,d).<sup>15,34,35</sup> The construction of heterogeneously coupled optical cavities is another approach for single-mode operation. Analogous to the Vernier effect,<sup>13,14</sup> the coupling of the two optical cavities can effectively enhance the gain of a specific mode while suppressing other modes (Figure 1e), thus achieving single-mode lasing output.<sup>7</sup> However, these strategies inevitably bring energy absorption and scattering and promote laser thresholds. Other abovementioned strategies based on microfabrication technologies are not suitable for organic crystals due to the manufacturing difficulty of organic materials. Here, we propose a unique approach for the single-mode laser from the large-dimensional organic crystals by means of BICs from the composite structure consisting of nanowires and PhCs (Figure 1b,f).

The organic nanowires of (*E*)-6-methoxy-3-(((4-nitrophenyl)imino)methyl)-2*H*-chromene-4-olate-BF<sub>2</sub> (MOON)<sup>36</sup> are chosen as a model for the subsequent research studies. Their synthesis and structural and spectral characterization are described in detail in the Supporting Information (Figures S3 and S4). Figure 2a shows a schematic of the preparation process of the composite system. The obtained samples are characterized by scanning electron microscopy (SEM) and are shown in Figure 2b. Clearly, a MOON nanowire with a typical length of about 100  $\mu\text{m}$  lies flat on 3D PhC, which shows the symmetric triangular lattice of the spherical silica (SiO<sub>2</sub>) spheres. This nanowire exhibits bright photoluminescence (PL) and an excellent optical waveguide with a low propagation loss of 0.0082 dB/ $\mu\text{m}$  (Figure S5).

We perform power-dependent PL measurement using the homemade micro-PL setup (Figure S6) for the collection of lasing signals. The NWs were uniformly pumped by a 400 nm femtosecond laser beam, which is chosen as a pump light and its waist is adjusted to be larger than the nanowire length. To characterize the BIC in the composite system, we first perform the spatially resolved PL measurements (see details in the Supplementary methods). As shown in Figure 2d, the PL

spectra from location 1 (black circle in Figure 2b) and location 2 of the nanowire display the same maximum emission band at 585 nm, which is consistent with the PL of the whole nanowire (Figure S4). Notably, the PL spectrum from location 1 has one shoulder peak at 655 nm more than that from location 2. This is characteristic evidence of a BIC because that the PL at certain wavelengths (the filled area of a red color) can be enhanced and confined in the nanowire due to the existence of the BIC. Therefore, the PL spectrum from the edge of the nanowire shows significant enhancement. We also measure the control experiments on the sample of the nanowire on the ordinary glass substrate. The PL spectra from the two locations show no evident differences (Figure S7).

We characterize the laser behaviors of the MOON nanowire on the PhC substrate with the glass substrate as the control sample. The obvious multimode lasing emission (black line in Figure 2e), with the threshold of 4.28  $\mu\text{J}/\text{cm}^2$  (black line in Figure 2f), is observed in the sample of glass substrates. In strong contrast, an excellent single-mode operating laser (red line in Figure 2e) is achieved from the sample of the PhC substrate and its threshold decreases significantly to 0.41  $\mu\text{J}/\text{cm}^2$  (red line in Figure 2f), which is approximately 10 times lower than that of the sample of the glass substrate. Meanwhile, the super linear increase of PL intensities with  $p = 11.35 \pm 0.01$  above the threshold indicates the typical laser emission. The side-mode suppression ratio of nanowire laser (3D PhC) is 20 dB (Figure S9). In summary, the single-mode laser generated by the hybrid system of a 3D PhC substrate coupled with organic one-dimensional (1D) nanowires exhibits outstanding performance characteristics.

The PhC substrate and organic crystals form a composite structure, which, compared to a glass substrate, can provide periodic scattering for the optical modes within the organic crystal and form a hybrid BIC, thus achieving mode selection. In the presence of this scattering, only the optical modes that are perfectly bound within the organic crystal, i.e., the hybrid BIC of the composite system, can achieve stable gain and lasing. Note that in the experiments, the 3D PhC substrates

were prepared by the self-assembly method, and defects inevitably existed. The existence of defects would cause the hybrid BIC in the composite structure to be broken into a quasi-BIC.<sup>23</sup> While, the quasi-BIC can still exhibit a higher  $Q$  factor compared to other modes and continues to support single-mode lasing. Therefore, the results obtained through our proposed method demonstrate a certain level of robustness in single-mode lasing. In fact, BIC can widely exist in periodic photonic systems.<sup>17–19</sup> To give an easier and clearer perspective of the proposed BIC-based single-mode nanowire lasers, we also present another simple composite system composed of nanowire and 1D PhC grating.<sup>37</sup>

As shown in Figure 3a, the substrate is a 1D PhC grating, whose period  $a$  is 278 nm. The 1D PhC grating is along the  $x$  direction, and the angle between the nanowire's length and the  $x$  direction is  $\theta$ . As the angle  $\theta$  increases, the effective period of periodic scattering along the nanowire direction by the grating will also increase accordingly. The effective period can be estimated by  $a/\cos \theta$ . When the  $\theta$  angle is  $\theta_1$  ( $\sim 0^\circ$ ), at which angle the effective period is about 278 nm, we collect single-mode lasing emission at a wavelength of 635 nm. In contrast, as  $\theta$  angle increased to  $\theta_2$  ( $\sim 19.5^\circ$ ), at which angle the effective period is about 295 nm, multimode emission emerged. To reveal the differences of two lasing performances, we calculated TM-like photonic bands of two effective composite systems with different periodically scatterings, as is shown in Figure 3c. For the simulation setups, see the Supplementary Methods. For composite system 1 ( $\theta_1$ ), we mark the at- $\Gamma$  BIC (green point) and an off- $\Gamma$  optical mode (gray point) in the photonic bands, whose  $x$ -component electric field distributions are exhibited in the left panel of Figure 3d. For the at- $\Gamma$  BIC, the light field is confined in the nanowire, corresponding to an ultrahigh  $Q$  factor. In contrast, for the off- $\Gamma$  optical mode, the light in the nanowire can be scattered into the free space, corresponding to a relatively low  $Q$  factor. The BIC locates in the lasing wavelength range of the organic crystal nanowire, leading to the final single-mode lasing. For the composite system 2 ( $\theta_2$ ), the wavelength of the BIC is out of the lasing wavelength range of the organic crystal nanowire; hence, the lasing exhibited multimode emission. Additionally, similar PL measurements in Figure 2c were performed for two 1D PhC composite structures, as shown in Figure 3e,f. The measured additional PL peaks agree well with the calculated BIC of the effective composite systems. The consistency between the experiment and theoretical calculations confirmed the BIC origin of the single-mode laser.

In our proposed BIC-based single-mode laser, the lasing wavelength depends on the BIC mode, whose wavelength can be effectively modulated by the PhC period. By changing the period of the substrate, we can easily control the single-mode lasing wavelength of organic nanowires. We prepared PhC substrates using SiO<sub>2</sub> spheres of different diameters; as the diameter of the SiO<sub>2</sub> spheres increases from 265 to 286 nm (Figure S10), the wavelength of the single-mode laser also shifts from 639 to 657 nm (Figure 4a). In the 1D PhC composite structures, by increasing the angle  $\theta$  from  $0^\circ$  to  $15^\circ$ , the effective period can also be modulated, and the wavelength of the single-mode laser shifts from 635 to 656 nm, indicating a similar red-shift (Figure 4b). These results demonstrated the wavelength degree of freedom in our proposed BIC-based single lasers in the PhC-nanowire system. This work also provides the basis for the realization of laser displays based on PhC.<sup>38</sup>

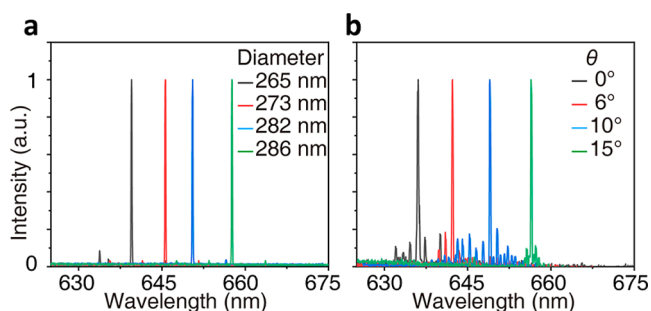


**Figure 4.** (a) Single-mode laser spectroscopy of nanowires on spherical SiO<sub>2</sub> substrates with different diameters. (b) Single-mode laser spectroscopy of nanowires on grating substrates with different  $\theta$ .

### 3. CONCLUSION

In summary, we demonstrate a low-threshold and robust single-mode laser based on BICs in the composite system consisting of an organic nanowire and PhC. This mechanism enables the realization of single-mode lasers in large-sized organic nanowires without the need for complex manipulations and structural designs while also effectively reducing the laser threshold. Benefited from the tunability of PhCs, the wavelength of single-mode laser can be effectively regulated due to the pronounced periodicity-dependent characteristics of BICs. Importantly, this device exhibits robust single-mode laser due to the immunity of the defects of 3D PhCs. This study not only contributes to the advancement of the organic single-mode laser technology but also provides a new application of BICs for lasers, paving the way for further applications of organic lasers.

### ■ ASSOCIATED CONTENT

#### Data Availability Statement

The data that support the plots within this paper and other findings of this study are available from the corresponding author upon reasonable request.

#### Supporting Information

The Supporting Information is available free of charge at <https://pubs.acs.org/doi/10.1021/acsp Photonics.5c02055>.

Experimental details, synthesis, characterization, device fabrication, and theoretical studies (PDF)

### ■ AUTHOR INFORMATION

#### Corresponding Authors

**Chunling Gu** – College of New Materials and Chemical Engineering, Beijing Institute of Petrochemical Technology, Beijing 102617, China; [orcid.org/0000-0002-3799-3275](https://orcid.org/0000-0002-3799-3275); Email: [clgu@bipt.edu.cn](mailto:clgu@bipt.edu.cn)

**Hongbing Fu** – Beijing Key Laboratory for Optical Materials and Photonic Devices Department of Chemistry, Capital Normal University & Beijing Advanced Innovation Center for Imaging Theory and Technology, Beijing 100048, P. R. China; [orcid.org/0000-0003-4528-189X](https://orcid.org/0000-0003-4528-189X); Email: [hbfu@cnu.edu.cn](mailto:hbfu@cnu.edu.cn)

**Lei Shi** – State Key Laboratory of Surface Physics, Key Laboratory of Micro- and Nano-Photonic Structures (Ministry of Education) and Department of Physics, Fudan University, Shanghai 200433, P. R. China; Email: [lshi@fudan.edu.cn](mailto:lshi@fudan.edu.cn)

**Qing Liao** – Beijing Key Laboratory for Optical Materials and Photonic Devices Department of Chemistry, Capital Normal

University & Beijing Advanced Innovation Center for Imaging Theory and Technology, Beijing 100048, P. R. China; [orcid.org/0000-0002-9169-4196](https://orcid.org/0000-0002-9169-4196); Email: [liaoqing@cnu.edu.cn](mailto:liaoqing@cnu.edu.cn)

## Authors

**Yuan Li** – Beijing Key Laboratory for Optical Materials and Photonic Devices Department of Chemistry, Capital Normal University & Beijing Advanced Innovation Center for Imaging Theory and Technology, Beijing 100048, P. R. China

**Jiajun Wang** – State Key Laboratory of Surface Physics, Key Laboratory of Micro- and Nano-Photonic Structures (Ministry of Education) and Department of Physics, Fudan University, Shanghai 200433, P. R. China

**Kai Wang** – Beijing Key Laboratory for Optical Materials and Photonic Devices Department of Chemistry, Capital Normal University & Beijing Advanced Innovation Center for Imaging Theory and Technology, Beijing 100048, P. R. China

Complete contact information is available at:

<https://pubs.acs.org/10.1021/acsp Photonics.Sc02055>

## Author Contributions

<sup>†</sup>Y.L. and J.W. contributed equally to this work. Q.L. and L.S. conceived the basic idea and designed the experiments. Y.L., J.W., and K.W. performed experimental measurements. J.W. and L.S. performed the theoretical simulations. C.G., H.F., L.S., and Q.L. wrote the manuscript with contributions from all authors. H.F. and Q.L. supervised the project. All authors analyzed the data and discussed the results.

## Funding

This work was supported by the National Natural Science Foundation of China (Grant Nos. 22090022, 22275125, 22150005, T2394480, T2394481, 12321161645, and 12234007), the National Key R&D Program of China (2022YFA1204402, 2018YFA0704805, and 2018YFA0704802), the Natural Science Foundation of Beijing, China (KZ202110028043), the Science and Technology Innovation Program of Hunan Province (2022RC4039), the Beijing Advanced Innovation Center for Imaging Theory and Technology.

## Notes

The authors declare no competing financial interest.

## REFERENCES

- (1) Yang, H.; Khayrudinov, V.; Dhaka, V.; Jiang, H.; Autere, A.; Lipsanen, H.; Sun, Z.; Jussila, H. Nanowire network-based multifunctional all-optical logic gates. *Sci. Adv.* **2018**, *4*, No. eaar7954.
- (2) Tournié, E.; Monge Bartolome, L.; Rio Calvo, M.; Loghmari, Z.; Diaz-Thomas, D. A.; Teissier, R.; Baranov, A. N.; Cerutti, L.; Rodriguez, J.-B. Mid-infrared III–V semiconductor lasers epitaxially grown on Si substrates. *Light: Sci. Appl.* **2022**, *11*, 165.
- (3) Piccione, B.; Cho, C. H.; van Vugt, L. K.; Agarwal, R. All-optical active switching in individual semiconductor nanowires. *Nat. Nanotechnol.* **2012**, *7*, 640–645.
- (4) Yu, Z.; Wu, Y.; Liao, Q.; Zhang, H.; Bai, S.; Li, H.; Xu, Z.; Sun, C.; Wang, X.; Yao, J.; Fu, H. Self-Assembled Microdisk Lasers of Perylene-3,4,9,10-tetracarboxylic diimides. *J. Am. Chem. Soc.* **2015**, *137*, 15105–15111.
- (5) Liao, Q.; Jin, X.; Zhang, H.; Xu, Z.; Yao, J.; Fu, H. An Organic Microcavity Laser Array Based on a Lateral Microcavity of a Single J-aggregation Microbelt. *Angew. Chem., Int. Ed.* **2015**, *54*, 7037–7041.
- (6) Dong, H.; Zhang, C.; Liu, Y.; Yan, Y.; Hu, F.; Zhao, Y. S. Organic Microcrystal Vibronic Lasers with Full-Spectrum Tunable

Output beyond the Franck–Condon Principle. *Angew. Chem., Int. Ed.* **2018**, *57*, 3108–3112.

(7) Wei, G.-Q.; Wang, X.-D.; Liao, L.-S. Recent Advances in 1D Organic Solid-State Lasers. *Adv. Funct. Mater.* **2019**, *29*, 1902981.

(8) Huang, H.; Yang, L.; He, J.; Yang, Y.; Yao, J.; Liao, Q.; Fu, H. Two-Dimensional Organic Crystals Enabling Anisotropic Photon Transport and Dual-Color Orthogonally Polarized Laser. *Adv. Opt. Mater.* **2023**, *11* (13), 2202797.

(9) Clark, J.; Lanzani, G. Organic photonics for communications. *Nat. Photonics* **2010**, *4*, 438–446.

(10) Feng, L.; Wong, Z. J.; Ma, R. M.; Wang, Y.; Zhang, X. Single-mode laser by parity-time symmetry breaking. *Science* **2014**, *346*, 972–975.

(11) Hodaei, H.; Miri, M. A.; Heinrich, M.; Christodoulides, D. N.; Khajavikhan, M. Parity-time-symmetric microring lasers. *Science* **2014**, *346*, 975–978.

(12) Zhang, C.; Shu, F.-J.; Zou, C.-L.; Dong, H.; Yao, J.; Zhao, Y. S. Organic Synthetic Photonic Systems with Reconfigurable Parity–Time Symmetry Breaking for Tunable Single-Mode Microlasers. *Adv. Mater.* **2023**, *35*, 2300054.

(13) Zhang, C.; Zou, C.-L.; Dong, H.; Yan, Y.; Yao, J.; Zhao, Y. S. Dual-color single-mode lasing in axially coupled organic nanowire resonators. *Sci. Adv.* **2017**, *3*, No. e1700225.

(14) Gao, H.; Fu, A.; Andrews, S. C.; Yang, P. Cleaved-coupled nanowire lasers. *Proc. Natl. Acad. Sci. U.S.A.* **2013**, *110*, 865–869.

(15) Ma, R. M.; Oulton, R. F.; Sorger, V. J.; Bartal, G.; Zhang, X. Room-temperature sub-diffraction-limited plasmon laser by total internal reflection. *Nat. Mater.* **2011**, *10*, 110–113.

(16) Hill, M. T.; Oei, Y.-S.; Smalbrugge, B.; Zhu, Y.; de Vries, T.; van Veldhoven, P. J.; van Otten, F. W. M.; Eijkemans, T. J.; Turkiewicz, J. P.; de Waardt, H.; Geluk, E. J.; Kwon, S.-H.; Lee, Y.-H.; Nötzel, R.; Smit, M. K. Lasing in metallic-coated nanocavities. *Nat. Photonics* **2007**, *1*, 589–594.

(17) Nakamura, M.; Aiki, K.; Umeda, J.; Yariv, A. cw operation of distributed-feedback GaAs-GaAlAs diode lasers at temperatures up to 300 K. *Appl. Phys. Lett.* **1975**, *27*, 403–405.

(18) Kogelnik, H.; Shank, C. V. Coupled-Wave Theory of Distributed Feedback Lasers. *J. Appl. Phys.* **1972**, *43*, 2327–2335.

(19) Yang, L.; Li, G.; Gao, X.; Lu, L. Topological-cavity surface-emitting laser. *Nat. Photonics* **2022**, *16*, 279–283.

(20) Gao, X.; Yang, L.; Lin, H.; Zhang, L.; Li, J.; Bo, F.; Wang, Z.; Lu, L. Dirac-vortex topological cavities. *Nat. Nanotechnol.* **2020**, *15*, 1012–1018.

(21) Hsu, C. W.; Zhen, B.; Stone, A. D.; Joannopoulos, J. D.; Soljačić, M. Bound states in the continuum. *Nat. Rev. Mater.* **2016**, *1*, 16048.

(22) Kang, M.; Liu, T.; Chan, C. T.; Xiao, M. Applications of bound states in the continuum in photonics. *Nat. Rev. Mater.* **2023**, *5*, 659–678.

(23) Wang, J.; Li, P.; Zhao, X.; Qian, Z.; Wang, X.; Wang, F.; Zhou, X.; Han, D.; Peng, C.; Shi, L.; Zi, J. Optical bound states in the continuum in periodic structures: mechanisms, effects, and applications. *Photon Insights* **2024**, *3*, R01–R26.

(24) Qin, H.; Su, Z.; Liu, M.; Zeng, Y.; Tang, M.-C.; Li, M.; Shi, Y.; Huang, W.; Qiu, C.-W.; Song, Q. Arbitrarily polarized bound states in the continuum with twisted photonic crystal slabs. *Light: Sci. Appl.* **2023**, *12*, 66.

(25) Hsu, C. W.; Zhen, B.; Lee, J.; Chua, S. L.; Johnson, S. G.; Joannopoulos, J. D.; Soljačić, M. Observation of trapped light within the radiation continuum. *Nature* **2013**, *499*, 188–191.

(26) Zhong, H.; Yu, Y.; Zheng, Z.; Ding, Z.; Zhao, X.; Yang, J.; Wei, Y.; Chen, Y.; Yu, S. Ultra-low threshold continuous-wave quantum dot mini-BIC lasers. *Light: Sci. Appl.* **2023**, *12*, 100.

(27) Kühner, L.; Wendisch, F. J.; Antonov, A. A.; Bürger, J.; Hüttenhofer, L.; de S Menezes, L.; Maier, S. A.; Gorkunov, M. V.; Kivshar, Y.; Tittel, A. Unlocking the out-of-plane dimension for photonic bound states in the continuum to achieve maximum optical chirality. *Light: Sci. Appl.* **2023**, *12*, 250.

(28) Kodigala, A.; Lepetit, T.; Gu, Q.; Bahari, B.; Fainman, Y.; Kanté, B. Lasing action from photonic bound states in continuum. *Nature* **2017**, *541*, 196–199.

(29) Ha, S. T.; Fu, Y. H.; Emani, N. K.; Pan, Z.; Bakker, R. M.; Paniagua-Domínguez, R.; Kuznetsov, A. I. Directional lasing in resonant semiconductor nanoantenna arrays. *Nat. Nanotechnol.* **2018**, *13*, 1042–1047.

(30) Yu, Y.; Sakanas, A.; Zali, A. R.; Semenova, E.; Yvind, K.; Mørk, J. Ultra-coherent Fano laser based on a bound state in the continuum. *Nat. Photonics* **2021**, *15*, 758–764.

(31) Ren, Y.; Li, P.; Liu, Z.; Chen, Z.; Chen, Y. L.; Peng, C.; Liu, J. Low-threshold nanolasers based on miniaturized bound states in the continuum. *Sci. Adv.* **2022**, *8*, No. eade8817.

(32) Huang, C.; Zhang, C.; Xiao, S.; Wang, Y.; Fan, Y.; Liu, Y.; Zhang, N.; Qu, G.; Ji, H.; Han, J.; Ge, Li.; Kivshar, Y.; Song, Q. Ultrafast control of vortex microlasers. *Science* **2020**, *367*, 1018–1021.

(33) Chen, Y.; Feng, J.; Huang, Y.; Chen, W.; Su, R.; Ghosh, S.; Hou, Y.; Xiong, Q.; Qiu, C. W. Compact spin-valley-locked perovskite emission. *Nat. Mater.* **2023**, *22*, 1065–1070.

(34) Zhang, C.; Zou, C. L.; Yan, Y.; Hao, R.; Sun, F. W.; Han, Z. F.; Zhao, Y. S.; Yao, J. Two-Photon Pumped Lasing in Single-Crystal Organic Nanowire Exciton Polariton Resonators. *J. Am. Chem. Soc.* **2011**, *133*, 7276–7279.

(35) Wang, X.; Liao, Q.; Li, H.; Bai, S.; Wu, Y.; Lu, X.; Hu, H.; Shi, Q.; Fu, H. Near-Infrared Lasing from Small-Molecule Organic Hemispheres. *J. Am. Chem. Soc.* **2015**, *137*, 9289–9295.

(36) Li, Y.; Wang, K.; Liao, Q.; Fu, L.; Gu, C.; Yu, Z.; Fu, H. Tunable Triplet-Mediated Multicolor Lasing from Nondoped Organic TADF Microcrystals. *Nano Lett.* **2021**, *21*, 3287–3294.

(37) Wright, J. B.; Campione, S.; Liu, S.; Martinez, J. A.; Xu, H.; Luk, T. S.; Li, Q.; Wang, G. T.; Swartzentruber, B. S.; Lester, L. F.; Brener, I. Distributed feedback gallium nitride nanowire lasers. *Appl. Phys. Lett.* **2014**, *104* (4), 041107.

(38) Liu, Y.; Hou, X.; Song, Y.; Li, M. Bioinspired reflective display based on photonic crystals. *Interdiscip. Mater.* **2024**, *3*, 54–73.



CAS BIOFINDER DISCOVERY PLATFORM™

**ELIMINATE DATA SILOS. FIND WHAT YOU NEED, WHEN YOU NEED IT.**

A single platform for relevant, high-quality biological and toxicology research

**Streamline your R&D**

**CAS**  
A division of the American Chemical Society

The advertisement features a vertical strip on the left showing a 3D molecular model with atoms represented by spheres in various colors (grey, red, blue, green) and bonds. The background is a dark blue gradient.